JACS
JOURNAL OF THE AMERICAN CHEMICAL SOCIETY
Article
pubs.acs.org/JACS

Trade-off between Processivity and Hydrolytic Velocity of Cellobiohydrolases at the Surface of Crystalline Cellulose

Akihiko Nakamura,[†,‡] Hiroki Watanabe,[§,‡] Takuya Ishida,[†,∥] Takayuki Uchihashi,[§,⊥,#] Masahisa Wada,[†,▽] Toshio Ando,[§,⊥,#] Kiyohiko Igarashi,[†,∥] and Masahiro Samejima*[,†]

[†]Department of Biomaterial Sciences, Graduate School of Agricultural and Life Sciences, The University of Tokyo, Yayoi, Bunkyo-ku, Tokyo 113-8657, Japan

[§]Department of Physics, Kanazawa University, Kakuma-machi, Kanazawa 920-1192, Japan

[∥]Advanced Low Carbon Technology Research and Development Program, Japan Science and Technology Agency, Goban-cho, Chiyoda-ku, Tokyo 102-0076, Japan

[⊥]Bio-AFM Frontier Research Center, College of Science and Engineering, Kanazawa University, Kakuma-machi, Kanazawa 920-1192, Japan

[#]Core Research for Evolutional Science and Technology, Japan Science and Technology Agency, Sanbon-cho, Chiyoda-ku, Tokyo102-0075, Japan

[▽]Department of Plant and Environmental New Resources, College of Life Sciences, Kyung Hee University, Seocheon-dong, Giheung-ku, Yongin-si, Gyeonggi-do 446-701, Republic of Korea

Supporting Information

ABSTRACT: Analysis of heterogeneous catalysis at an interface is difficult because of the variety of reaction sites and the difficulty of observing the reaction. Enzymatic hydrolysis of cellulose by cellulases is a typical heterogeneous reaction at a solid/liquid interface, and a key parameter of such reactions on polymeric substrates is the processivity, i.e., the number of catalytic cycles that can occur without detachment of the enzyme from the substrate. In this study, we evaluated the reactions of three closely related glycoside hydrolase family 7 cellobiohydrolases from filamentous fungi at the molecular level by means of high-speed atomic force microscopy to investigate the structure−function relationship of the cellobiohydrolases on crystalline cellulose. We found that high moving velocity of enzyme molecules on the surface is associated with a high dissociation rate constant from the substrate, which means weak interaction between enzyme and substrate. Moreover, higher values of processivity were associated with more loop regions covering the subsite cleft, which may imply higher binding affinity. Loop regions covering the subsites result in stronger interaction, which decreases the velocity but increases the processivity. These results indicate that there is a trade-off between processivity and hydrolytic velocity among processive cellulases.

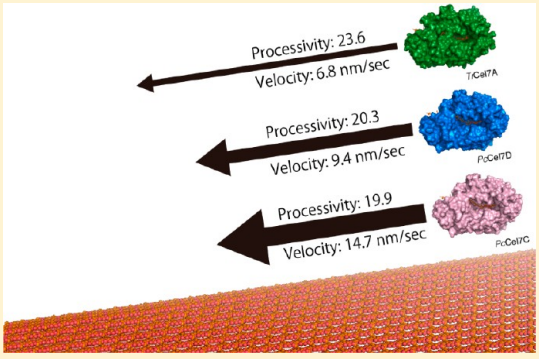

INTRODUCTION

Although homogeneous catalysis has been extensively studied, heterogeneous catalysis is less well understood because of the variety of the reaction sites and the difficulty of observing the reaction.[1] Among biochemical reactions, enzyme reactions at a solid/liquid interface with an insoluble substrate are particularly intractable. The reasons for this include the complexity of solid surfaces, which makes it difficult to know how much of the enzyme is catalytically active, and differences in the mobility of the enzyme molecules on the surface. In the case of polymeric substrates, which are common in nature, a key parameter is the processivity, which is the number of catalytic cycles that can occur without detachment of the enzyme from the substrate.[2,3] Processivity is difficult to evaluate biochemically. However, we recently used high-speed atomic force microscopy (HS-AFM) to visualize the behavior of single molecules of cellulase during hydrolysis of crystalline cellulose.[4] This technique enables direct measurement of the processivity and catalytic velocity of enzyme molecules without the need for enzyme labeling or substrate modification.

Cellulose, the main structural polysaccharide of plant cell walls, is the most abundant biopolymer on Earth. In nature, cellulose chains, linear polymers of β-1,4-linked D-glucose units, are packed into ordered arrays to form crystalline cellulose I.[5] Because cellulose chains have stable β-glycosidic bonds[6] and each chain is also stabilized by intra- and intermolecular hydrogen bonds in the crystal,[7] cellulose I is quite resistant not only to chemical hydrolysis but also to enzymatic degradation. When cellulose I is treated by ammonia, however, the crystal

Received: November 24, 2013
Published: February 26, 2014

   dx.doi.org/10.1021/ja4119994 | J. Am. Chem. Soc. 2014, 136, 4584−4592

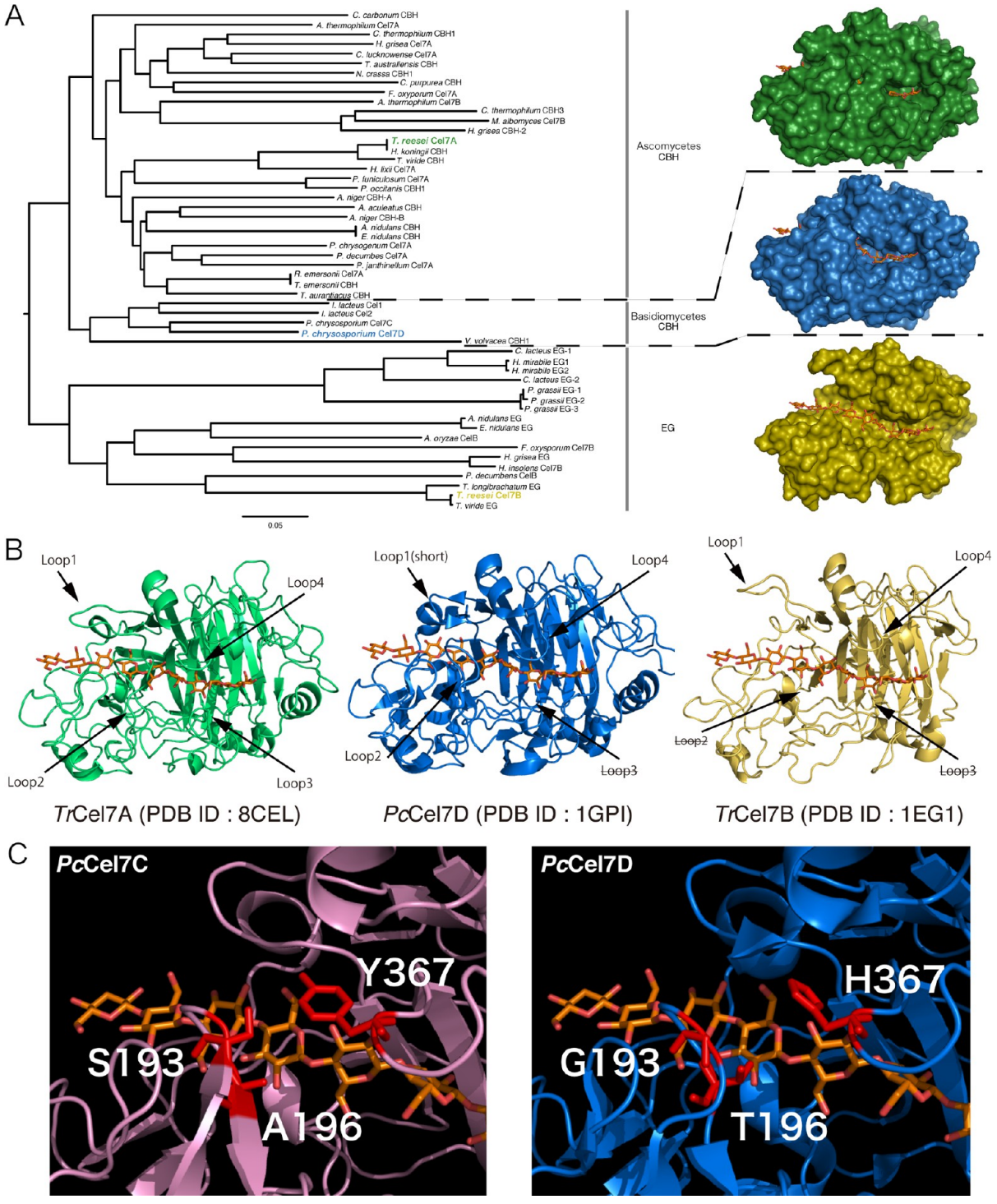

Figure 1. (A) Phylogenetic tree of the sequence-based alignment of Cel7s classified as "characterized" by CAZY (http://www.cazy.org/). Sequences were aligned and the tree was made with ClustalW2 server default settings. X-ray crystal structures of Cel7s and comparison of their overall structures. Green, *Tr*Cel7A (8CEL); blue, *Pc*Cel7D (1GPI); yellow, *Tr*Cel7B (1EG1). Orange, Superimposed cellulose chain in enzyme subsite. (B) Differences of loop regions. *Tr*Cel7A has four loop regions (loop1 to loop4), and *Pc*Cel7D has loop2, loop4, and a short loop1 region. *Tr*Cel7B lacks loop2 and loop3. Orange, superimposed cellulose chain in enzyme subsite. (C) Different amino acids around the loop regions between *Pc*Cel7C and *Pc*Cel7D. Y367 and H367 residues are located on loop4, and the others are located on loop2.

transforms into cellulose III_I,[8] which is easily degraded by cellulase than cellulose I.[9]

Cellulolytic microorganisms secrete a set of cellulases, cellobiohydrolases (CBHs: EC 3.2.1.91 and EC 3.2.1.176) and endoglucanases (EGs: EC 3.2.1.4), to degrade cellulose.[10] In the cellulose degradation system of the ascomycetes fungus *Trichoderma reesei*, a dominant component of the secreted proteins is glycoside hydrolase (GH) family 7 cellobiohydrolase (*Tr*Cel7A, formerly known as CBH I), which produces cellobiose from the reducing end of cellulose.[11−13] *Tr*Cel7A has a two-domain structure,[14] with a catalytic domain (CD) and a cellulose-binding domain (CBD) belonging to the

dx.doi.org/10.1021/ja4119994 | J. Am. Chem. Soc. 2014, 136, 4584−4592

carbohydrate-binding module (CBM) family 1. These domains are connected by a highly *O*-glycosylated linker region. The CD has a β-sandwich structure, formed by β-strands connected with α-helices and loop regions stabilized by many disulfide bridges, and contains substrate-binding sites for 10 glucose units (subsites −7 to +3).[15] The CBD in *Tr*Cel7A consists of only 35 amino acids, being rather small compared with the CD, which has a molecular weight of ∼50 kDa.[16]

The wood-rotting basidiomycete *Phanerochaete chrysosporium* is one of the best-studied cellulolytic filamentous fungi, together with *T. reesei*. The total genome of this fungus was sequenced by the Joint Genome Institute (http://genome.jgi-psf.org/Phchr1/Phchr1.home.html),[17−19] and the data show that *P. chrysosporium* has seven genes coding Cel7 isozymes (Cel7A−Cel7F/G).[19,20] Because the pattern of gene expression varies depending on the conditions of cultivation, the gene products (Cel7s) are assumed to have distinct roles.[21−25] Among them, *Pc*Cel7C and *Pc*Cel7D (formerly known as CBH62 and CBH58, respectively[26]) are the major secretory proteins in cellulolytic culture, accounting for up to 80% of extracellular proteins. *Pc*Cel7D was first identified as a homologue of *Tr*Cel7A from *P. chrysosporium*.[27,28] *Pc*Cel7C has higher carboxymethyl cellulose-degrading activity than *Pc*Cel7D.[26] The X-ray structure of *Pc*Cel7D was solved, and a homology model of *Pc*Cel7C was compared with *Pc*Cel7D based on the high amino acid sequence identity of the catalytic domains (81%).[29] The comparison of the X-ray structure and the homology model indicated that the overall fold is the same between the two enzymes, but three amino acids in the catalytic tunnel are different in *Pc*Cel7C from those in *Pc*Cel7D (Figure 1).

On the basis of the X-ray structure of the catalytic core of *Tr*Cel7A, which revealed a tunnel-like subsite structure constructed from loop regions, the reaction of GH7 CBH was suggested to be processive.[30] *Tr*Cel7A and *Pc*Cel7D are likely to show different processivity because of the difference in the number of loop regions covering the subsite.[31,32] However, measurement of processivity is difficult because of the variety of enzyme-binding states on cellulose. In the present study, we compared *Pc*Cel7C, *Pc*Cel7D, and *Tr*Cel7A in terms of moving velocity on the substrate and half-life of the movement in order to characterize the structure−function relationship GH family 7 CBHs.

EXPERIMENTAL PROCEDURES

Cultivation of *Phanerochaete chrysosporium*. *P. chrysosporium* strain K-3 was grown on 2 L of Kremer and Wood medium containing 2% cellulose (CF11; Whatman) as the sole carbon source in a jar fermenter with 5 L working volume (Takasugi Seisakusho, Tokyo, Japan). The temperature was 37 °C, and the pH was maintained at 5.0 with phosphoric acid and potassium hydroxide. Stirring was done at 300 rpm, and air was supplied at 2.0 L/min. After cultivation for 5 days, the culture supernatant was separated using a glass filter membrane. Extracellular proteins were precipitated with ammonium sulfate at 70% saturation and stored at 4 °C.

Purification of Enzymes. Precipitated extracellular proteins were dissolved in 20 mM potassium phosphate buffer (pH 7.0) and applied to a DEAE-Toyopearl 650S column (TOSOH, Tokyo, Japan; column volume (CV) = 150 mL) equilibrated with 20 mM potassium phosphate buffer (pH 7.0) after desalting. Proteins were eluted with a linear gradient of 0−300 mM KCl in 1050 mL. Protein concentration of fractions was estimated with a Protein Assay kit (Bio-Rad, Hercules, CA) according to the manufacturer's instructions. Aliquots of 20 μL were incubated with 20 μL of 10 mM *p*-nitrophenyl lactoside (*p*NPL), 20 μL of 1.0 M sodium acetate buffer (pH 5.0), and 140 μL of water. The reaction was stopped by the addition of 20 μL of 2.0 M Na_2CO_3, and the absorbance of the reaction mixture was measured at 405 nm (Abs_{405} = 16.6 mM^{-1} cm^{-1}). *p*NPL-hydrolyzing activity (units) was calculated using the standard curve of *p*-nitrophenol. The purity of each fraction was checked by SDS-PAGE, and fractions containing proteins of about 58 and 62 kDa proteins with *p*NPL-hydrolyzing activity were collected. The 62 kDa protein in flow-through fractions was equilibrated with 20 mM Tris-HCl buffer, pH 8.0, and applied to a SuperQ-Toyopearl 650S (TOSOH; CV = 100 mL) equilibrated with the same buffer. Elution was done with a linear gradient of 0−0.1 M NaCl in 800 mL of 20 mM Tris-HCl, pH 8.0. Next, ammonium sulfate was added to the protein solution to a final concentration of 1.0 M, and fractionation was carried out on a Phenyl-Toyopearl 650S column (CV = 67 mL) equilibrated with 20 mM sodium acetate buffer (pH 5.0) containing 1.0 M ammonium sulfate. Proteins were eluted with a reverse linear gradient of 1.0 to 0 M ammonium sulfate in 134 mL. Finally, the protein solution was equilibrated with 20 mM Tris-HCl buffer (pH 8.0) and fractionated on a DEAE-Toyopearl 650S column (CV = 150 mL) equilibrated with the same buffer. Proteins were eluted with a linear gradient of 0−50 mM NaCl in 1350 mL. The fractions were assayed as described above, and fractions containing 62 kDa protein with *p*NPL-hydrolyzing activity were collected and equilibrated with 20 mM sodium acetate buffer (pH 5.0). The 58 kDa protein solution was similarly fractionated on a Phenyl-Toyopearl 650S column (TOSOH; CV = 67 mL). Finally, the protein solution was equilibrated with 20 mM potassium phosphate buffer (pH 7.0). Elution was done with a linear gradient of 0−50 mM KCl in 1350 mL. The fractions were assayed as described above, and 58 kDa protein-containing fractions with *p*NPL-hydrolyzing activity but without *p*-nitrophenylbitrophenyl-β-D-glucoside-hydrolyzing activity were collected and equilibrated with 20 mM sodium acetate buffer, pH 5.0, by an ultrafiltration.

*Tr*Cel7A was purified from Celluclast 1.5L (Novozymes, Denmark). The crude enzyme was desalted by a gel filtration column (TOYOPEARL HW-40S; TOSOH; CV = 45 mL), which was equilibrated with 20 mM potassium phosphate buffer pH 7.0. The protein concentrations of each fraction were measured by a Protein Assay kit, and the fractions containing protein were mixed and injected into an anion-exchange column (TOYOPEARL DEAE-650S, CV = 150 mL), which was equilibrated with the same buffer. The proteins were eluted by a linear gradient up to 300 mM KCl. After the measurement of protein concentration, the *p*NPL-hydrolyzing activity was measured, and the purity of each fraction was estimated by SDS-PAGE. The fractions containing ∼60 kDa enzyme, which has activity for *p*NPL, were collected and mixed with the same volume of 2.0 M ammonium sulfate solution to a final concentration of 1.0 M. The enzyme solution was injected to a hydrophobic interaction column (TOYOPEARL Phenyl-650S; CV = 67 mL), which was equilibrated with 20 mM of sodium acetate buffer, pH 5.0, containing 1.0 M ammonium sulfate. The enzyme was eluted by a linear reverse gradient of ammonium sulfate to 0 M. The protein concentration, activity for *p*NPL, and purity of each fraction were analyzed by the same methods, and the enzyme was collected. The buffer solution of the enzyme was changed to 20 mM of sodium acetate buffer, pH 5.0.

The enzyme solutions were filtrated by a polyvinylidene fluoride (PVDF) membrane with 0.1 μm pore size (Ultrafree Centrifugal Filters, Merch-Millpore, Deutschland). The purity of the three enzymes was checked by SDS-PAGE analysis on 12% polyacrylamide gel. The contamination of endoglucanase was estimated as <1% (mol/mol) from the viscometric measurement of carboxymethyl cellulose (CMC) degrading as shown in Figure S2 of the Supporting Information.

Cellulose Preparation. Highly crystalline cellulose I_α and III_I were prepared according to a previous report.[33] Phosphoric acid-swollen cellulose (PASC) was prepared from Avicel (Funakoshi, Tokyo, Japan). Avicel was dissolved in 85% (w/w) phosphoric acid, and the solution was made completely clear by vigorous agitation with a glass stick. After overnight incubation at 4 °C, cellulose was regenerated in water and homogenized in a high-speed blender. The cellulose suspension was washed with water and stored at 4 °C.

dx.doi.org/10.1021/ja4119994 | J. Am. Chem. Soc. 2014, 136, 4584−4592

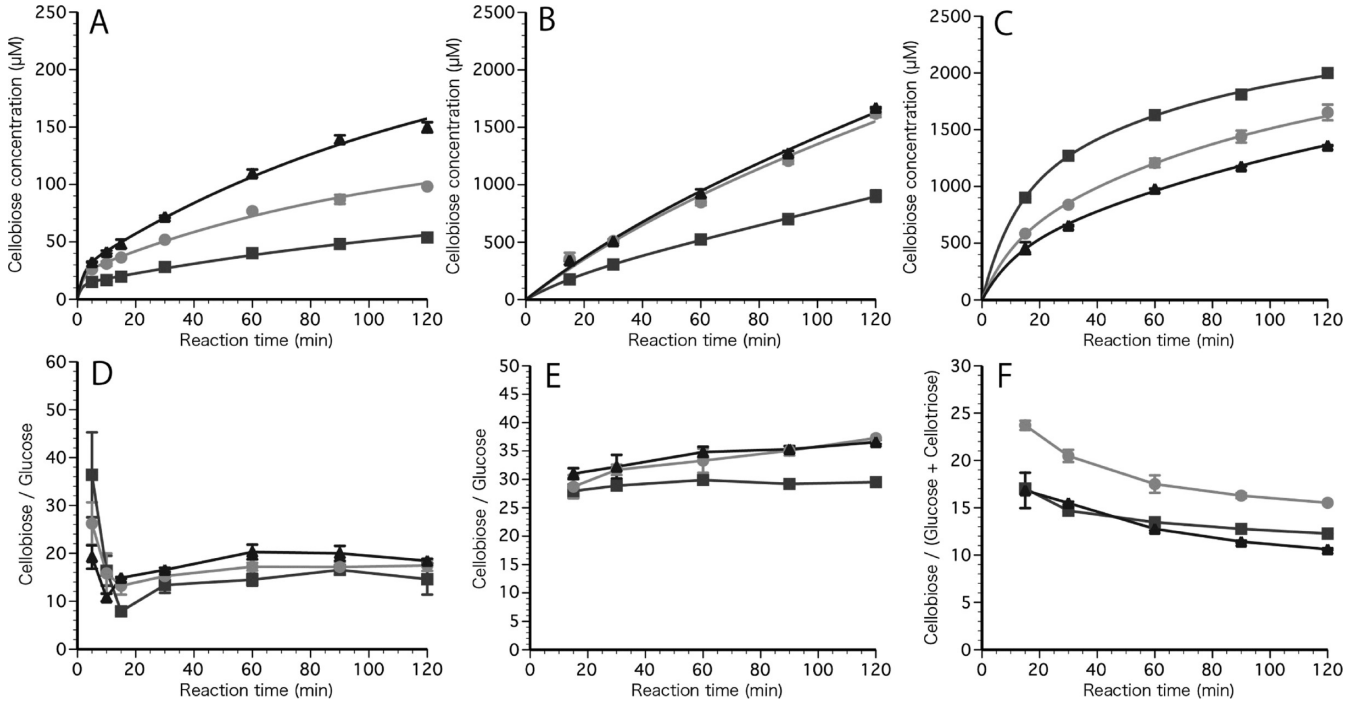

Figure 2. Time course of products formation (top) and ratio of cellobiose/glulose + cellotriose (bottom) formed from crystalline cellulose I_α (A, D), cellulose III_I (B, E), and PASC (C, F). Cellulose (0.1%) was incubated with 2.0 μM enzymes in 50 mM sodium acetate buffer, pH 5.0, at 30 °C. Triangle, *Tr*Cel7A; square, *Pc*Cel7C; circle, *Pc*Cel7D. Error bars show standard deviation (SD) and are from the three independent measurements.

Activity Measurement. Purified *Tr*Cel7A, *Pc*Cel7C, and *Pc*Cel7D (2.0 μM) were each incubated with 0.1% cellulose I_α, cellulose III_I, or PASC in 50 mM sodium acetate buffer, pH 5.0, at 30 °C. After 15, 30, 60, 90, and 120 min incubation (additionally 5 and 10 min incubation for cellulose I_α), the reaction mixture was filtered using MultiScreen 0.22 μm filter plates (Millipore, Billerica, MA) and products were separated and quantified by high-performance liquid chromatography (HPLC; JASCO LC-2000) on a NH2-P column (Showa Denko K. K., Kanagawa, Japan) with a Corona-CAD detector (ESA Biosciences, Chelmsford, MA). Concentrations of cellobiose in the reaction mixtures, $q(t)$, were fitted to the equations

$$q(t) = a\cdot(1 - \exp(-b\cdot t)) + c\cdot(1 - \exp(-d\cdot t)) \quad (1)$$

for cellulose I_α and PASC and

$$q(t) = a\cdot(1 - \exp(-b\cdot t)) + c\cdot t \quad (2)$$

for cellulose III_I, where a, b, c, and d are constants and t is the incubation time. Equation 1 and eq 2 were differentiated to eqs 3 and 4, respectively, for the estimation of the velocity of cellobiose production as follows:

$$v(t) = a\cdot b\exp(-b\cdot t) + c\cdot d\exp(-d\cdot t) \quad (3)$$

$$v(t) = a\cdot b\exp(-b\cdot t) + c \quad (4)$$

These functions are semiempirical and just used to calculate the velocity of cellobiose production. The ratio of cellobiose/glulose + cellotriose production was estimated according to the previous report.[31]

HS-AFM Observation. Movements of molecules of the three cellulases on the substrate surface were observed by HS-AFM based on the previous reports.[4,34,35] Histograms of averaged velocities of individual molecules during one processive reaction were drawn using IGOR Pro 6 (WaveMetrics, Portland, OR) and fitted to a Gaussian distribution. Moving times of molecules were calculated from the number of frames in which the molecules were observed, and plots of the number of molecules in each range of moving time were fitted to the equation

$$f(t) = a_0\exp\left(-\frac{\ln 2}{\tau}\cdot t\right) \quad (5)$$

where a_0 is the intercept of the y-axis, τ is the half-life of the processive movement, and t is duration time. In eq 5, $(\ln 2/\tau)$ is the dissociation constant of the moving-enzyme (k_{off}) (the detail is available as Supporting Information). For the HS-AFM experiments, highly crystalline cellulose III_I was used as a substrate to obtain enough numbers of molecules for statistical analysis.

RESULTS

General Characteristics of Cel7s. After five days of cultivation, ~2 g of crude enzymes were produced, and approximately 300 and 600 mg of *Pc*Cel7C and *Pc*Cel7D, respectively, were purified with sufficient purity for the present experiments. After several steps of column chromatography, *Pc*Cel7C, *Pc*Cel7D, and *Tr*Cel7A were each homogeneous on SDS-PAGE as shown in Figure S2 of the Supporting Information. The purified enzymes were incubated with crystalline cellulose I_α, III_I, and PASC, and the amounts of products were measured by HPLC. The progress curves are shown in Figure 2A–C. The major product was cellobiose, whereas glucose was detected from all of the substrates and cellotriose was produced from PASC. *Tr*Cel7A produced cellobiose from cellulose I_α with the highest velocity among three CBHs (1.1 ± 0.1 μM/min at 60 min), whereas those of *Pc*Cel7D and *Pc*Cel7C were 0.63 ± 0.01 and 0.35 ± 0.03 μM/min at 60 min, respectively. When cellulose III_I was used, the velocity of cellobiose production by *Tr*Cel7A was similar to that of *Pc*Cel7D, whereas *Pc*Cel7C was less active toward cellulose III_I, as shown in Figure 2B. In contrast, *Pc*Cel7C produced cellobiose faster than *Pc*Cel7D and *Tr*Cel7A when PASC was used as a substrate. In the degradation of PASC, the velocity of cellobiose production by *Pc*Cel7C was 17.2 ± 1.1 μM/min at 30 min of incubation, which is 1.2 times faster than that of

dx.doi.org/10.1021/ja4119994 | J. Am. Chem. Soc. 2014, 136, 4584–4592

Table 1. Summary of Biochemical Measurement and AFM Observations

	biochemical measurement[a]						AFM observation			
	velocity of cellobiose production (μM/min)			ratio of cellobiose/glulose + cellotriose						
enzyme	cellulose I_α	cellulose III_I	PASC	cellulose I_α	cellulose III_I	PASC	dissociation rate constant[b] (s^{-1})	half-life of movement[b] (s)	averaged velocity[c] (nm/s)	half-life processivity[d]
*Pc*Cel7C	0.35 ± 0.03	6.6 ± 0.6	17.2 ± 1.1	14.5 ± 1.2	29.9 ± 0.1	14.7 ± 0.1	0.51 ± 0.01	1.4 ± 0.0	14.7 ± 9.1	19.9
*Pc*Cel7D	0.63 ± 0.01	12.2 ± 0.3	14.6 ± 1.4	17.2 ± 0.8	33.3 ± 2.1	20.5 ± 0.6	0.32 ± 0.04	2.2 ± 0.1	9.4 ± 3.7	20.3
*Tr*Cel7A	1.1 ± 0.1	12.7 ± 0.1	11.9 ± 2.2	20.3 ± 1.5	34.8 ± 0.9	15.5 ± 0.1	0.20 ± 0.01	3.5 ± 0.2	6.8 ± 3.5	23.6

[a]The values of cellulose I_α and cellulose III_I were at 60 min incubation, and the values of PASC were at 30 min incubation. The values are mean ± standard deviation. [b]The mean ± SE of the fitting with the exponential decay. [c]The mean ± SD with the Gaussian. [d]Half life processivity = half-life period (s) × averaged velocity (nm/s)/cellobiose length (nm) = ln(2) × processivity.

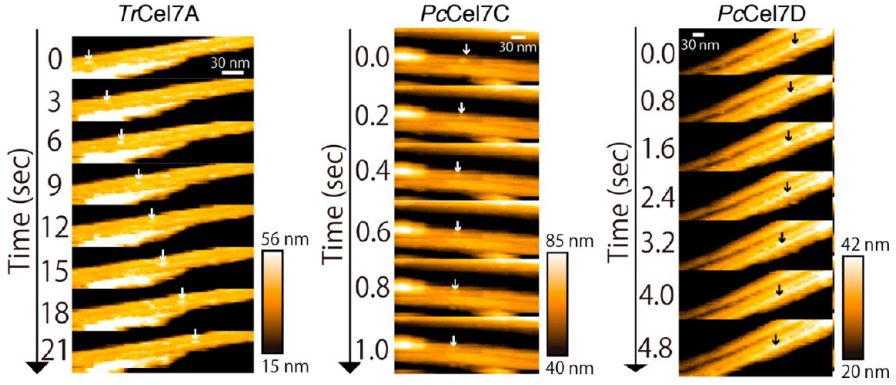

Figure 3. High-speed AFM images of the three CBHs. Positions of each enzyme molecule are marked by rectangles. Enzyme (0.55 μM) was observed in 50 mM NaAc buffer, pH 5.0, at 25 °C. Frame rate was 0.2 frame/s.

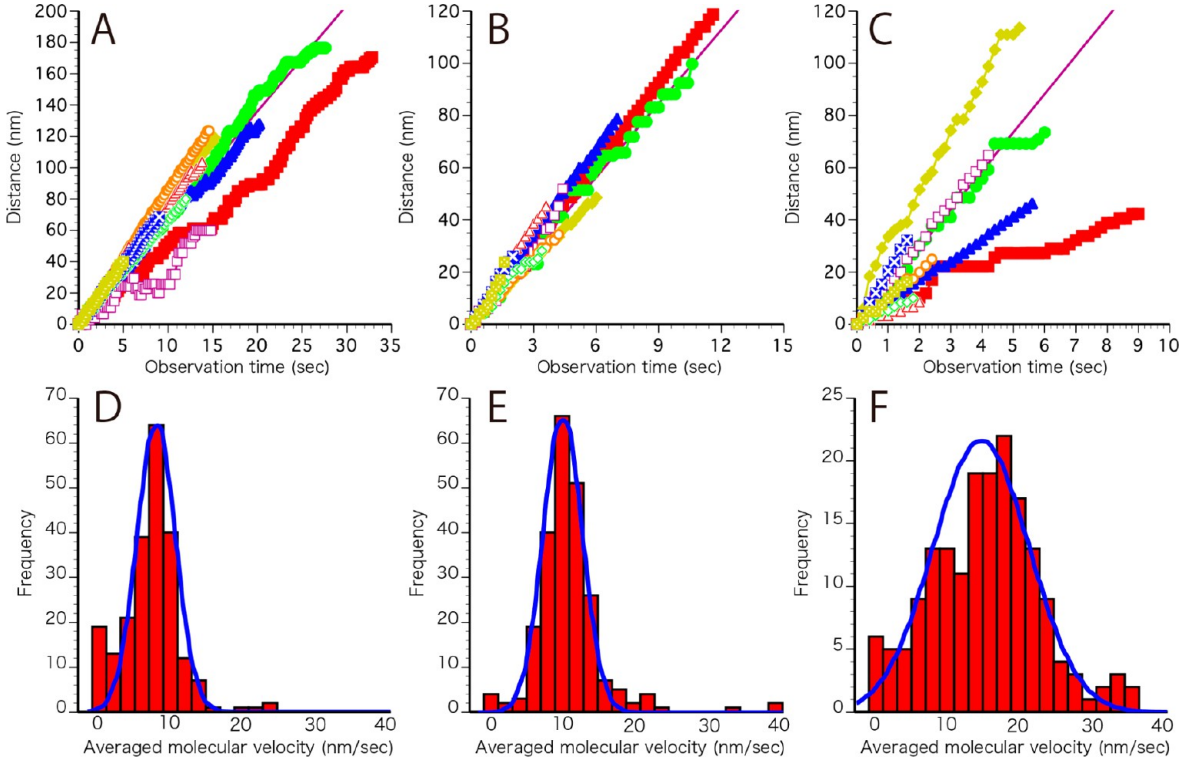

Figure 4. Examples of movement characteristics and averaged velocity histograms of *Tr*Cel7A (A, D), *Pc*Cel7D (B, E), and *Pc*Cel7C (C, F). Averaged velocities were calculated from the moving-distances and duration of each molecule. Peak values in each Gaussian distribution (D–F) are indicated by lines in the corresponding upper figures (A–C).

*Pc*Cel7D (14.6 ± 1.4 μM/min) and 1.4 times faster than that of *Tr*Cel7A (11.9 ± 2.2 μM/min). The ratio of cellobiose/glucose + cellotriose in cellulose I_α degradation was 20.3 ± 1.5 for *Tr*Cel7A, 17.2 ± 0.8 for *Pc*Cel7D, and 14.5 ± 1.2 for *Pc*Cel7C at 60 min of incubation. These values were relatively higher using cellulose III_I, and 34.8 ± 0.9 for *Tr*Cel7A, 33.3 ± 2.1 for

dx.doi.org/10.1021/ja4119994 | J. Am. Chem. Soc. 2014, 136, 4584–4592

*Pc*Cel7D, and 29.9 ± 0.1 for *Pc*Cel7C. In the case of PASC degradation, *Pc*Cel7D showed the highest value (20.5 ± 0.6 at 30 min), and *Tr*Cel7A and *Pc*Cel7C showed the values of 14.7 ± 0.1 and 15.5 ± 0.1, respectively. These values are summarized in Table 1.

HS-AFM Observation for the Statistic Analysis of Processive Movement. *Tr*Cel7A, *Pc*Cel7C, and *Pc*Cel7D molecules moving on the surface of crystalline cellulose were observed by HS-AFM (Figure 3A−C). Many moving molecules were detected in all cases, although the velocity of the movement and the duration varied, as shown in Movies S3−S5 in Supporting Information and Figure 4A−C. The movements were then analyzed statistically to quantify the differences. The movement of *Tr*Cel7A molecules showed a Gaussian distribution with mean ± SD of 6.8 ± 3.5 nm/s (n = 220, Figure 4D), whereas those of *Pc*Cel7D and *Pc*Cel7C were 9.4 ± 3.7 nm/s (n = 233, Figure 4E) and 14.7 ± 9.1 nm/s (n = 176, Figure 4F), respectively. The longest movement was observed for *Tr*Cel7A with ∼250 nm, whereas those of *Pc*Cel7C and *Pc*Cel7D were ∼120 nm (Figure S6 in Supporting Information). When the duration of the movements was analyzed, the graphs were fitted to a single exponential decay for all three CBHs. The values of half-life ± standard error (SE) (τ) of *Tr*Cel7A, *Pc*Cel7D, and *Pc*Cel7C were 3.5 ± 0.2, 2.2 ± 0.1, and 1.4 ± 0.0 s, respectively. In addition, the values of dissociation rate constant ± SE (k_{off}) of *Tr*Cel7A, *Pc*Cel7D, and *Pc*Cel7C were 0.20 ± 0.01, 0.32 ± 0.04, and 0.51 ± 0.01 s^{-1}, respectively.

DISCUSSION

The structures of several GH family 7 cellulases (CBHs and EGs) have been solved, and the structure−function relationship between CBH and EG can be understood in terms of these structures, i.e., CBHs contain rather closed, tunnel-shaped active sites, whereas EGs lack the loops that cover the subsites in CBHs and exhibit cleft-type active sites. This difference is clearly reflected in the phylogenetic tree (Figure 1A) of GH family 7 cellulases, 35 CBHs and 17 EGs. At the sequence level, GH family 7 cellulases are initially divided into two categories, CBH and EG. The clade of CBH was further divided into two nodes, representing ascomycete and basidiomycete CBHs. Representative X-ray crystal structures of the three groups are shown in Figure 1A. Ascomycete CBHs have four loop regions, two of which are absent in EGs, and the subsites of EGs are more open than those of CBHs (Figure 1 B). Basidiomycete CBHs lack one of the loops (loop3) covering the active site compared with ascomycete CBHs. Therefore, the active-site structure of basidiomycete CBHs is intermediate between those of ascomycete CBHs and EGs. Comparison of processivity among these enzymes is expected to show how these structural characteristics influence the processive reaction of GH7 CBHs. It is well-known that ascomycete *T. reesei* produces CBH (*Tr*Cel7A) and EG (*Tr*Cel7B) in cellulose-grown culture medium, whereas basidiomycete *P. chrysosporium* mainly produces two similar CBHs, *Pc*Cel7C and *Pc*Cel7D. *T. reesei* degrades cellulose by synergistic action between CBH-type and EG-type of GH7 enzyme (*Tr*Cel7A and *Tr*Cel7B).[36] In contrast, basidiomycetes such as *P. chrysosporium* have no apparent EG-type Cel7, indicating that basidiomycete employ a different ratio of enzymes from ascomycete to degrade cellulose. Therefore we compared the CBHs from *P. chrysosporium* and *T. reesei* by the biochemical measurements and HS-AFM observations in order to characterize the structure−function relationship.

HS-AFM can observe single molecules moving on a cellulose surface with catalysis.[4,34,35] Here, we observed many molecules moving on the surface of crystalline cellulose for all three CBHs (Figure 3), and the results indicated that *Pc*Cel7C and *Pc*Cel7D are processive enzymes as well as *Tr*Cel7A, indicating that the regions of loop2 and loop4 are important but loop3 is not necessary for processive reaction of CBH on crystalline cellulose. Using cellulose III_I, we were able to observe enough molecules for statistical analysis and comparison of the three CBHs. The moving velocity of *Tr*Cel7A on crystalline cellulose III_I obtained in the present study (6.8 ± 3.5 nm/s) was almost the same as that on crystalline cellulose I_α (7.1 ± 3.9 nm/s) as reported previously,[34] indicating that the conversion of crystalline from I_α to III_I does not affect the velocity of the processive movement. Therefore we compared the movement of the three CBHs on crystalline cellulose III_I. Among the three CBHs, the values of averaged hydrolytic velocities of *Pc*Cel7C and *Pc*Cel7D were higher than that of *Tr*Cel7A. In the present work, we also analyzed the duration of processive movements of CBH molecules on crystalline cellulose in order to calculate the half-life of their movements. From the values of hydrolytic velocities and the values of half-life of processive movements, we calculated the half-life processivity of the three CBHs (Table 1). The half-life processivity of *Tr*Cel7A was higher than the values of *Pc*Cel7C and *Pc*Cel7D. This result from the single-molecule observation well shows that the tunnel-like structure of GH family 7 CBH is important for the processivity as reported before.[31] Among three enzymes, only *Tr*Cel7A contains the loop3 region, which includes amino acids interacting with the cellulose chain at subsites −2 (Y247), +1 (T246, R251), and +2 (R251). This may imply that *Tr*Cel7A has stronger affinity for the cellulose chain, and this could be the reason why the processivity of *Tr*Cel7A was higher than those of the other two CBHs. It was reported that the catalytic domain of *Tr*Cel7A has more favorable binding free energy than that of *Pc*Cel7D.[37] Therefore, it is implied that the stability of the complex between CD and cellulose chain is important for the processive reaction. The more loops covering the active site causes higher processivity of cellobiohydrolase but lower hydrolytic velocity.

Comparison of *Pc*Cel7C and *Pc*Cel7D showed no difference in the amino acids that are expected to interact directly with the cellulose chain in the subsites of the catalytic domains.[29] The CBDs of these enzymes are also very similar, and only one amino acid, which is not located at the binding surface, is different. Thus, there is a high overall degree of similarity between these two enzymes. However, three amino acids constructing loop regions of tunnel-like structure are different. They are located in loop2 and loop4 covering the active-site tunnel as shown in Figure 1C. Gly193, Thr196, and His367 in *Pc*Cel7D are replaced by Ser, Ala, and Tyr, respectively, in *Pc*Cel7C, and it has been predicted that the changes at loop2 (G193S and T196A) make the loop more flexible.[29] Although the structures of *Pc*Cel7C and *Pc*Cel7D only differ around subsites −4 and −3, the two enzymes exhibit different velocities of hydrolysis and different affinities for the cellulose chain. This result suggests that the higher flexibility of loop2 is related to the faster velocity of the processive reaction.

When the parameters of the three CBHs obtained by HS-AFM observations were compared, *Pc*Cel7D moved slower than *Pc*Cel7C, but it had a longer moving-duration than

dx.doi.org/10.1021/ja4119994 | J. Am. Chem. Soc. 2014, 136, 4584−4592

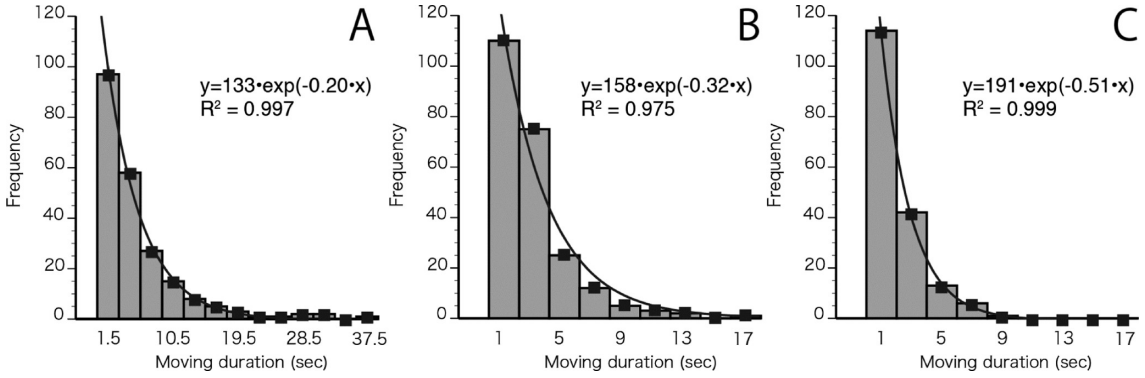

Figure 5. Histograms of moving-durations. A, *Tr*Cel7A; B, *Pc*Cel7D; C, *Pc*Cel7C. Moving-durations were calculated from the number of frames in which each molecule was detected during tracking.

*Pc*Cel7C. In addition, *Tr*Cel7A moved much more slowly than *Pc*Cel7D and had a longer moving-duration than *Pc*Cel7D (Figure 5). The movements in HS-AFM observation involve catalysis, which has been confirmed by the immobility of the inactive mutant of *Tr*Cel7A (E212Q) in our previous study, indicating that the velocity of the movements is the velocity of the processive cycle when we analyze moving molecules on the surface of the substrate. On the other hand, moving-duration is an indicator of the stability of the complex between CD and cellulose chain. The relationship between velocity and moving-duration of the three CBHs suggests that higher stability of the complex hinders the moving on the cellulose. Recently it has been discussed that the rate-limiting step of the degradation of cellulose is a decrystallization process of the substrate.[38,39] Allthough we are unable to distinguish decrystallization of the substrate and the sliding movement of CD, because the sliding movement should promote decrystallization of cellulose, while the decrystallization should cause movement vice versa, we speculate that the rate-limiting step of crystalline cellulose degradation is the process rather than the catalysis as discussed from "bulk" experiments.[38,39]

Although a direct comparison between the results of single-molecule observation and biochemical activity measurement is often difficult, the order of hydrolytic activity on PASC was the same as the order of the velocity of processive movement and k_{off}. This result implies that the rate-limiting step of PASC hydrolysis is the catalytic process or the off-rate from the substrate, but not decided by processivity. This is supported by the report that a less processive mutant of chitinase hydrolyzes chitosan faster than does wild-type chitinase.[40] In addition, because PASC contains large numbers of cellulose chain ends and free chains for the initiation of endotype hydrolysis,[32] capturing the substrate chain by CD or decrystallization of the substrate is not a rate-limiting step.[41] In the hydrolysis of crystalline cellulose I_α, the relationship among the three enzymes was similar to that of processivity whereas the difference between *Pc*Cel7D and *Tr*Cel7A was smaller in cellulose III_I hydrolysis. The big difference between the two crystalline celluloses is the shape of the crystal. Cellulose III_I has large hydrophobic surface and more numbers of accessible chain ends for CBHs than cellulose I_α.[34] These results may imply that the bottleneck of crystalline cellulose degradation is the process of picking up a chain-end. Processivity is determined as the balance between two kinetic parameters, k_{cat} and k_{off}, which determines how many catalytic cycles occur per binding episode of the catalytic domain. Therefore, it is reasonable that processivity is more important for the degradation of crystalline cellulose, which has less accessible chain ends.

The velocity of processive movement estimated from the HS-AFM observation and the velocities of cellobiose production determined by biochemical experiments were very different as reported previously[4,34] (Table 1). Considering only reactive (working) enzyme molecules are visualized in the HS-AFM observation and biochemical bulk experiments cause underestimation of the specific activity of the CBHs, the number of active enzymes was quite limited (<1% of added enzyme) at the surface of the crystalline cellulose. In contrast, the processivity obtained from the ratio of cellobiose/glulose + cellotriose in the biochemical experiment reflects the processivity estimated from the HS-AFM observation more than we expected, suggesting that the biochemical estimation is effective to know the rough value of processivity for CBHs. The similarity between the values of processivity estimated from the HS-AFM observation and the ratio of cellobiose/glulose + cellotriose indicates the ratio cancels the amount of nonworking enzyme. The processivity of *Tr*Cel7A was previously reported as ∼60 for the degradation of bacterial cellulose,[32,42] which is about twice the value determined by HS-AFM observation in this study (k_{cat}/k_{off} = 34). We think the major reason of the difference is the difference of the substrate and/or different techniques to estimate the value. We are now determining the processivity and k_{off} by the different single molecular methods, such as a fluorescence microscope in addition to recently developed HS-AFM combined with single-molecule fluorescence microscope.[43] Although the absolute value of processivity is still open for discussion, we may have to use the same substrate prepared by the same protocol to compare the processivity.

In applications of cellulases for degradation of biomass, the substrate will contain both crystalline and amorphous regions. From the comparison among *Tr*Cel7A, *Pc*Cel7C, and *Pc*Cel7D in this study, higher processivity is better for the degradation of the crystalline region of the cellulose, whereas higher hydrolytic activity by higher dissociation rate constant is better for the degradation of the amorphous region. Therefore, the suitable enzyme may differ depending upon the crystallinity of cellulose in biomass. Moreover, the contribution of the processivity becomes smaller when the substrate is treated chemically, because decrease of degree of polymerization causes an increase of accessible chain-ends of the substrate, which also occurred by the reaction of other enzymes in the enzyme cocktail such as EGs and redox enzymes. We believe that the present findings will be helpful to select CBHs for industrial cellulosic biomass conversion.

dx.doi.org/10.1021/ja4119994 | *J. Am. Chem. Soc.* 2014, 136, 4584−4592

CONCLUSION

We used HS-AFM to evaluate the kinetic parameters for processive reaction of three cellobiohydrolases, as well as the relationship between processivity and the structure of the enzymes. The correlation between catalytic rate constant and dissociation rate constant indicated that higher affinity for the substrate causes a lower catalytic rate, which is a trade-off between processivity and hydrolytic velocity in cellobiohydrolases. Considering the higher processivity has the advantage in crystalline cellulose degradation and higher catalytic reaction has the advantage in hydrolysis of amorphous cellulose, this information is quite important for the design of enzyme cocktails for better hydrolysis of a cellulosic biomass.

ASSOCIATED CONTENT

Supporting Information

Additional results and details of methods described within the manuscript. Supplementary Movie S1, crystalline cellulose degradation movie of *Tr*Cel7A. Supplementary Movie S2, crystalline cellulose degradation movie of *Pc*Cel7D. Supplementary Movie S3, crystalline cellulose degradation movie of *Pc*Cel7C. This material is available free of charge via the Internet at http://pubs.acs.org.

AUTHOR INFORMATION

Corresponding Author

E-mail: amsam@mail.ecc.u-tokyo.ac.jp.

Author Contributions

‡These authors contributed equally.

Notes

The authors declare no competing financial interest.

ACKNOWLEDGMENTS

This research was supported by a grant for Development of an Innovative and Comprehensive Production System for Cellulosic Bioethanol to M.S. (09000833-0) from the New Energy and Industrial Technology Development Organization, by a grant from the Advanced Low Carbon Technology Research and Development Program (ALCA) of the Japan Science and Technology Agency (JST) to K.I., by Grants-in-Aid for Scientific Research for Young Scientists (A: No. 19688016 and 21688023) and (B: No. 17780245), by a Grant-in-Aid for Scientific Research (B: No. 24380089), and by a Grant-in-Aid for Innovative Areas (No. 24114008) to K.I. from the Japanese Ministry of Education, Culture, Sports, and Technology (MEXT) and Grant-in-Aid for JSPS Fellows to A.N. (25•7574) from Japan Society for the Promotion of Science (JSPS).

REFERENCES

(1) Ertl, G. *J. Mol. Catal. A: Chem.* **2002**, *182−183*, 5.
(2) Breyer, W. A.; Matthews, B. W. *Protein Sci.* **2001**, *10*, 1699.
(3) Horn, S. J.; Sørlie, M.; Vårum, K. M.; Valjamae, P.; Eijsink, V. G. H. *Methods Enzymol.* **2012**, *510*, 69.
(4) Igarashi, K.; Koivula, A.; Wada, M.; Kimura, S.; Penttilä, M.; Samejima, M. *J. Biol. Chem.* **2009**, *284*, 36186.
(5) Hon, D. N. S. *Cellulose* **1994**, *1*, 1.
(6) Wolfenden, R.; Yuan, Y. *J. Am. Chem. Soc.* **2008**, *130*, 7548.
(7) Nishiyama, Y.; Sugiyama, J.; Chanzy, H.; Langan, P. *J. Am. Chem. Soc.* **2003**, *125*, 14330.
(8) Wada, M.; Chanzy, H.; Nishiyama, Y.; Langan, P. *Macromolecules* **2004**, *37*, 8548.
(9) Igarashi, K.; Wada, M.; Samejima, M. *FEBS J.* **2007**, *274*, 1785.
(10) Lynd, L.; Weimer, P.; Van Zyl, W.; Pretorius, I. *Microbiol. Mol. Biol. Rev.* **2002**, *66*, 506.
(11) Ilmen, M.; Saloheimo, A.; Onnela, M.; Penttila, M. *Appl. Environ. Microbiol.* **1997**, *63*, 1298.
(12) Uusitalo, J.; Helena Nevalainen, K.; Harkki, A.; Knowles, J.; Penttilä, M. *J. Biotechnol.* **1991**, *17*, 35.
(13) Teeri, T. *Trends Biotechnol.* **1997**, *15*, 160.
(14) Abuja, P.; Schmuck, M.; Pilz, I.; Tomme, P.; Claeyssens, M.; Esterbauer, H. *Eur. Biophys. J.* **1988**, *15*, 339.
(15) Divne, C.; Stahlberg, J.; Reinikainen, T.; Ruohonen, L.; Pettersson, G.; Knowles, J.; Teeri, T.; Jones, T. *Science* **1994**, *265*, 524.
(16) Mattinen, M. L.; Kontteli, M.; Kerovuo, J.; Linder, M.; Annila, A.; Lindeberg, G.; Reinikainen, T.; Drakenberg, T. *Protein Sci.* **1997**, *6*, 294.
(17) Broda, P.; Birch, P.; Brooks, P.; Sims, P. *Mol. Microbiol.* **1996**, *19*, 923.
(18) Martinez, D.; Larrondo, L. F.; Putnam, N.; Gelpke, M. D. S.; Huang, K.; Chapman, J.; Helfenbein, K. G.; Ramaiya, P.; Detter, J. C.; Larimer, F.; Coutinho, P. M.; Henrissat, B.; Berka, R.; Cullen, D.; Rokhsar, D. *Nat. Biotechnol.* **2004**, *22*, 695.
(19) Wymelenberg, A.; Minges, P.; Sabat, G.; Martinez, D.; Aerts, A.; Salamov, A.; Grigoriev, I.; Shapiro, H.; Putnam, N.; Belinky, P. *Fungal Genet. Biol.* **2006**, *43*, 343.
(20) Covert, S.; Bolduc, J.; Cullen, D. *Curr. Genet.* **1992**, *22*, 407.
(21) Covert, S.; Vanden Wymelenberg, A.; Cullen, D. *Appl. Environ. Microbiol.* **1992**, *58*, 2168.
(22) Lamar, R.; Schoenike, B.; Vanden Wymelenberg, A.; Stewart, P.; Dietrich, D.; Cullen, D. *Appl. Environ. Microbiol.* **1995**, *61*, 2122.
(23) Vallim, M.; Janse, B.; Gaskell, J.; Pizzirani-Kleiner, A.; Cullen, D. *Appl. Environ. Microbiol.* **1998**, *64*, 1924.
(24) Sato, S.; Feltus, F. A.; Iyer, P.; Tien, M. *Curr. Genet.* **2009**, *55*, 273.
(25) Vanden Wymelenberg, A.; Gaskell, J.; Mozuch, M.; Kersten, P.; Sabat, G.; Martinez, D.; Cullen, D. *Appl. Environ. Microbiol.* **2009**, *75*, 4058.
(26) Uzcategui, E.; Ruiz, A.; Montesino, R.; Johansson, G.; Pettersson, G. *J. Biotechnol.* **1991**, *19*, 271.
(27) Eriksson, K.; Pettersson, B. *Eur. J. Biochem.* **1975**, *51*, 213.
(28) Sims, P.; James, C.; Broda, P. *Gene* **1988**, *74*, 411.
(29) MunÄoz, I.; Ubhayasekera, W.; Henriksson, H.; SzaboÂ, I.; Pettersson, G.; Johansson, G.; Mowbray, S.; Ståhlberg, J. *J. Mol. Biol.* **2001**, *314*, 1097.
(30) Davies, G.; Henrissat, B. *Structure* **1995**, *3*, 853.
(31) von Ossowski, I.; Ståhlberg, J.; Koivula, A.; Piens, K.; Becker, D.; Boer, H.; Harle, R.; Harris, M.; Divne, C.; Mahdi, S. *J. Mol. Biol.* **2003**, *333*, 817.
(32) Kurasin, M.; Valjamae, P. *J. Biol. Chem.* **2011**, *286*, 169.
(33) Wada, M.; Chanzy, H.; Nishiyama, Y.; Langan, P. *Macromolecules* **2004**, *37*, 8548.
(34) Igarashi, K.; Uchihashi, T.; Koivula, A.; Wada, M.; Kimura, S.; Okamoto, T.; Penttila, M.; Ando, T.; Samejima, M. *Science* **2011**, *333*, 1279.
(35) Igarashi, K.; Uchihashi, T.; Koivula, A.; Wada, M.; Kimura, S.; Penttilä, M.; Ando, T.; Samejima, M. *Methods Enzymol.* **2012**, *510*, 169.
(36) Teeri, T.; Koivula, A.; Linder, M.; Wohlfahrt, G.; Divne, C.; Jones, T. *Biochem. Soc. Trans.* **1998**, *26*, 173.
(37) Payne, C. M.; Jiang, W.; Shirts, M. R.; Himmel, M. E.; Crowley, M. F.; Beckham, G. T. *J. Am. Chem. Soc.* **2013**, *135*, 18831.
(38) Chundawat, S. P.; Bellesia, G.; Uppugundla, N.; da Costa Sousa, L.; Gao, D.; Cheh, A. M.; Agarwal, U. P.; Bianchetti, C. M.; Phillips, J.; George, N.; Langan, P. *J. Am. Chem. Soc.* **2011**, *133*, 11163.
(39) Gao, D.; Chundawat, S. P.; Sethi, A.; Balan, V.; Gnanakaran, S.; Dale, B. E. *Proc. Natl. Acad. Sci. U.S.A.* **2013**, *110*, 10922.
(40) Horn, S. J.; Sikorski, P.; Cederkvist, J. B.; Vaaje-Kolstad, G.; Sørlie, M.; Synstad, B.; Vriend, G.; Vårum, K. M.; Eijsink, V. G. H. *Proc. Natl. Acad. Sci. U.S.A.* **2006**, *103*, 18089.
(41) Nakamura, A.; Tsukada, T.; Auer, S.; Furuta, T.; Wada, M.; Koivula, A.; Igarashi, K.; Samejima, M. *J. Biol. Chem.* **2013**, *288*, 13503.

(42) Jalak, J.; Kurasin, M.; Teugjas, H.; Valjamae, P. *J. Biol. Chem.* **2012**, *287*, 28802.
(43) Fukuda, S.; Uchihashi, T.; Iino, R.; Okazaki, Y.; Yoshida, M.; Igarashi, K.; Ando, T. *Rev. Sci. Instrum.* **2013**, *84*, 073706.